

Path integral molecular dynamics calculations of the H_6^+ and D_6^+ clusters on an ab initio potential energy surface

Akira Kakizaki,^a Toshiyuki Takayanagi,^{*a} Motoyuki Shiga^b

^aDepartment of Chemistry, Saitama University, 255 Shimo-Okubo, Sakura-ku, Saitama City, Saitama 338-8570, Japan

^bCenter for Computational Science and E-systems
Japan Atomic Energy Agency, Higashi-Ueno 6-9-3, Taito-ku, Tokyo 110-0015, Japan

Abstract

Path integral molecular dynamics simulations for the H_6^+ and D_6^+ cluster cations have been carried out in order to understand the floppy nature of their molecular structure due to quantum-mechanical fluctuation. A full-dimensional analytical potential energy surface for the ground electronic state of H_6^+ has been developed on the basis of accurate ab initio electronic structure calculations at the CCSD(T)/cc-pVTZ level. It is found that the outer $H_2(D_2)$ nuclei rotate almost freely and that the probability density distributions of the central $H_2(D_2)$ nuclei show strong spatial delocalization.

*Corresponding author. E-mail address: tako@chem.saitama-u.ac.jp

1. Introduction

The hydrogen cluster cation H_n^+ is the simplest cluster system containing only hydrogen atoms and has attracted considerable attention from both experimental and theoretical sides over the past years [1-16]. It has been well-known that the H_n^+ clusters are easily produced by electron bombardment or radiation-induced ionization of gaseous H_2 . In general, odd-membered H_n^+ cluster ions are mainly produced since the $H_2^+ + H_2 \rightarrow H_3^+ + H$ ion-molecule reaction is quite fast and the product triangular H_3^+ ion subsequently attracts neutral H_2 to form a larger cluster cation via three-body processes. Thus, all odd-membered H_n^+ cluster ions are known to have the H_3^+ -core structure. On the other hand, it has been shown that even-membered H_n^+ cluster cations are also produced in ionized H_2 gas although their yields are generally much smaller than those of the odd-membered H_n^+ clusters by a factor of 10^1 - 10^3 . Kirchner et al. [11] first observed the smallest H_4^+ cluster cation produced by the collision-induced dissociation of H_5^+ . In the subsequent work, Kirchner and Bowers [12] have succeeded in detecting H_4^+ , H_6^+ , H_8^+ , and H_{10}^+ as minor products of the H_n^+ cluster ion formation using a sophisticated high-resolution mass-spectrometric technique. Very recently, Toennies and co-workers [13] have observed even-membered D_n^+ cluster ions up to $n = 18$ using a supersonic free-jet expansion technique although the signal intensities for $n = 16$ and 18 were extremely weak.

On the theoretical side, in an early ab initio molecular orbital study by Wright and Borkman [17], H_4^+ , H_6^+ , and H_8^+ were predicted to have a H_3^+ -core type structure, in which H and/or H_2 are bound to the H_3^+ ion through weak attractive interaction. However, Montgomery and Michels [18] have theoretically shown that H_6^+ has two isomers, a H_3^+ -core type with C_s symmetry and a H_2^+ -core type with D_{2d} symmetry. In this D_{2d} - H_6^+ cluster with a H_2^+ -core, two H_2 molecules are bound to the central H_2^+ core with strong charge transfer attractive interaction. They have found that the D_{2d} - H_6^+ structure is more stable than the former C_s - H_6^+ structure. Kurosaki and Takayanagi [19, 20] have found that the isomerization barrier from the C_s - H_6^+ isomer to the D_{2d} - H_6^+ isomer is very small using a reaction path analysis. Subsequently, they have

systematically studied structures of larger H_8^+ , H_{10}^+ , H_{12}^+ , and H_{14}^+ clusters and found that the structures having the H_6^+ core (or H_2^+ core) are more stable in energy than those of the corresponding H_3^+ -core clusters. In these larger cluster cations, neutral H_2 molecules are found to be bound to the H_6^+ core by weak van der Waals attractive interaction. These theoretical results were also confirmed by later ab initio calculations of Symons and Woolley [21] and of Lunell et al [22].

Very recently, Kumada et al. [23-25] have found that an electron-spin-resonance (ESR) spectrum newly observed in γ - or X-ray irradiated solid para-hydrogen can be assigned to the H_6^+ cluster ion with the D_{2d} structure. They have also carried out isotopic substitution experiments and then confirmed the validity of their spectral assignment [25]. In addition, it was concluded that two side-on H_2 molecules in H_6^+ almost freely and independently rotate around the molecular axis of the H_2^+ core even under solid hydrogen condition at very low temperature of ~ 4 K. This result was partly explained by a very small barrier height (~ 1.4 meV) for the internal rotation of side-on H_2 [20]. However, quantum tunneling rotation should play a key role since the barrier height is still larger than the thermal energy corresponding to temperature of 4 K.

As mentioned above, although static structures of the even-membered H_n^+ cluster ions have previously been studied using ab initio electronic structure calculations, their dynamical structures due to nuclear quantum effects have not yet been understood. Since the H_n^+ cluster ions consist of lightest hydrogen atoms, it may be interesting to study those structures from a quantum mechanical point of view. Here we report results of quantum-mechanical path-integral molecular dynamics calculations of the H_6^+ (D_6^+) cluster cation on an accurate ab initio potential energy surface and consider nuclear fluctuation effects of this molecule from a theoretical viewpoint.

2. Computational procedure

We have performed ~ 10000 -point CCSD(T)/cc-pVTZ calculations for the H_6^+

cluster cation using the MOLPRO 2002 program package [26] to obtain potential energy values for use in creating a full-dimensional potential energy surface. In an early stage of our electronic structure calculations, we have tried to use various theoretical levels including CCSD(T), MRCI, and CASPT2 as well as one-electron basis sets (cc-pVTZ, aug-cc-pVTZ, cc-pVQZ, aug-cc-pVQZ, and cc-pV5Z). As a result, we have found that the CCSD(T)/cc-pVTZ level is accurate enough for obtaining reliable potential energy values. In particular, we found that the inclusion of diffuse basis sets does not quantitatively affect the feature of the potential energy surface at all.

We examined various analytical functional forms for describing the potential energy surface of the H_6^+ cluster cation. As a result, we have found that the following simple functional form, consisting of combination of 15 two-body terms, is adequate to describe the important features of the H_6^+ potential energy surface.

$$\begin{aligned}
 V(r_1 \dots r_{15}) = & D_{e1} [1 - \exp\{-\alpha_1(r_1 - r_{1e})\}]^2 + D_{e2} \sum_{i=2}^5 [1 - \exp\{-\alpha_2(r_i - r_{2e})\}]^2 \\
 & + D_{e3} \sum_{i=6}^7 [1 - \exp\{-\alpha_3(r_i - r_{3e})\}]^2 + \sum_{i=8}^{11} c_1 \exp(-\beta_1 r_i) + \sum_{i=12}^{15} c_2 \exp(-\beta_2 r_i) + V_e
 \end{aligned} \tag{1}$$

In Eq. (1), attractive interaction is expressed by a standard Morse potential while simple exponential functions are used for describing repulsive forces. Here, r_i ($i = 1-15$) is the internuclear distance. Notice that this functional form has 14 parameters. It should be, however, emphasized that the present fit is semiglobal in that it does not describe the fragmentation process into $H_2^+ + H_2 + H_2$. The fitting parameters were determined by using the standard non-linear least square method. The obtained parameters are listed in Table 1.

The plots of potential energies as a function of an internal coordinate are presented in Fig. 1. It is clear that the energy profiles taken from the fitted surface are quite close to the original CCSD(T)/cc-pVTZ energy profiles. Table 2 compare harmonic vibrational frequencies at the D_{2d} minimum and at the D_{2h} transition state obtained from the fitted surface to the CCSD(T) frequencies, which was obtained

directly from ab initio calculations. The agreement between the two results is seen to be reasonably good. Previous ab initio values at the MP2/cc-pVTZ level of theory are also listed in Table 2 for comparison.

A standard imaginary-time path-integral molecular dynamics (PIMD) simulation [27] was performed to calculate thermal equilibrium structures of the H_6^+ and D_6^+ cluster ions on the ab initio potential energy surface developed as mentioned above. The quantum mechanical character of H(D) atoms are described by cyclic bead chains in the path-integral formalism. The present PIMD calculations were carried out in the standard Cartesian coordinates. The PIMD run was performed with $P = 200-600$ beads in the temperature range of $T = 4-10$ K in order to obtain numerically converged results. We found that 600 beads are necessary although computed results are not strongly dependent on the temperature at least in the range of $T = 4-10$ K. With time increment $\Delta t = 0.5-5$ au, the total time steps were ranged 10^5-10^6 . The massive Nose-Hoover chain technique in velocity Verlet algorithm was used to control the system temperature. The details of our computational method are also described in Refs. 28-30.

3. Results

Figs. 2a and 2b display three-dimensional perspective plots of the probability density functions of the H_6^+ and D_6^+ nuclei at $T = 4$ K, respectively. In these plots, the coordinate origin is fixed at the center of mass of the two outer H_2 (D_2) molecules and the line connecting two midpoints of the outer H_2 (D_2) is taken to be x axis. Also, the center of mass of the central H_2 (D_2) is projected onto the x - y plane so as that the rotational motions of the outer H_2 molecules can be clearly seen. Figs. 2c and 2d show the same density distributions but projected onto the y - z plane. It is clearly seen that the shape of the density distributions of the outer H_2 (D_2) molecules around the x -axis is nearly circular. This result suggests nearly full rotation of these nuclei. The probability distribution for H_6^+ is seen to be slightly broader than that for D_6^+ , but the

difference is not so noticeable in these perspective plots. Another interesting point is that the distribution of the central H₂ nuclei also shows strong spatial delocalization.

At this point, it should be important to comments on rotational angular momentum of the present PIMD simulations. As mentioned in a previous section, since the PIMD calculations were carried out with the standard Cartesian coordinates, there is possibility that the whole cluster system has non-zero rotational angular momentum. In order to check this, we have calculated the expectation value of total angular momentum of the whole cluster system as well as the expectation value of the angular momentum of the outer H₂ molecules around the central H-H axis. As a result, these values were calculated to be $0.02 \hbar^2$ and $0.01 \hbar^2$, respectively, and are very close to zero. This indicates that our PIMD sampling scheme does not give extra angular momenta.

In order to understand the isotope effect more quantitatively, one-dimensional probability distribution functions projected onto an appropriate coordinate are displayed in Fig. 3. Fig. 3a shows the probability distributions of the outer H₂ (D₂) nuclei as a function of the dihedral angle ϕ . As expected, two maxima are seen at $\phi = 90$ and 270 degrees, corresponding to the potential minima for the D_{2d} configuration. The difference in the H₆⁺ probability density at $\phi = 90^\circ$ and $\phi = 0^\circ$ (D_{2h} transition-state configuration) is estimated to be about 10 %, indicating that the distribution is not completely flat. Also, in the case of D₆⁺, the density difference at $\phi = 90^\circ$ and $\phi = 0^\circ$ is calculated to be about 20 %. Thus, it is found that the nuclear distribution for the H₆⁺ cluster is slightly more isotropic than that for D₆⁺. Although these values cannot easily be ignored, the present PIMD result qualitatively suggests that the outer H₂ (D₂) molecules rotate nearly freely. It may also be interesting to compare these density differences to the classical Boltzmann distribution $\exp(-\delta E/kT)$, where δE is the potential energy difference between $\phi = 90^\circ$ and $\phi = 0^\circ$. At $T = 4$ K, the value is estimated to be only 0.017 and the classical distribution considerably favors $\phi = 90^\circ$ configurations of outer H₂ (D₂) molecules. Therefore, we can safely conclude that the corresponding rotational motions are in the quantum mechanical regime.

It should be emphasized that the present PIMD result is in qualitative

agreement with the recent ESR study of Kumada and his co-workers [25]. They have measured ESR spectra of H_3D^+ , H_4D_2^+ , and H_2D_4^+ molecules and concluded that the outer hydrogen molecules rotate even in solid hydrogen at $T = 4$ K. Thus, it is suggested that H/D replacement does not largely affect the overall rotation dynamics of the H_6^+ cluster.

Fig. 3b displays the one-dimensional probability density of nuclei as a function of the displacement distance d , where d is the projected distance measured from the line connecting two midpoints of the outer H_2 (D_2). The distribution of the outer H_2 nuclei in H_6^+ is peaked at $d \sim 0.74 a_0$ with a width being about $0.19 a_0$. In the case of D_6^+ , the distribution is slightly narrower than H_6^+ and its width is about $0.14 a_0$. It is interesting to note that the probability density distributions for the central H_2 nuclei show a very spread behavior in the range of $d \sim 0-0.7 a_0$, as was already seen in Fig. 2. In order to rationalize the probability density distributions obtained from the PIMD simulations, in Fig. 4 we plot atomic displacement vectors for three low-frequency vibrational modes of H_6^+ at the D_{2d} minimum and D_{2h} transition-state configurations. Needless to say, the lowest-frequency modes (66.1 and $65.4 i \text{ cm}^{-1}$) correspond to the rotational mode of the outer H_2 molecules around the central H-H axis. The next two low-frequency modes ($\sim 350 \text{ cm}^{-1}$) mainly correspond to the translation motion of the central H_2 nuclei, combined with the motions of the outer H_2 nuclei. Thus, it is suggested that the strong spatial delocalization of the central $\text{H}_2(\text{D}_2)$ nuclei observed in the PIMD simulations attributes to these vibrational modes.

4. Conclusions

In this work, we first developed accurate ab initio potential energy surface of the H_6^+ cluster in full dimensions at the CCSD(T)/cc-pVTZ level of theory. We have demonstrated that the both H_6^+ and D_6^+ clusters have a very floppy nature due to quantum fluctuation using full-dimensional quantum PIMD simulations on the developed potential energy surface. The probability density distributions of the outer

H_2 (D_2) molecules show a unique behavior of nearly free rotation. This result is in qualitative agreement with the recent ESR experimental study of Kumada and co-workers [23-25]. In addition, it has been found that the density distribution of the central H_2 nuclei also show strong spatial delocalization. The result of the present PIMD simulations strongly indicates that quantum-mechanical treatment is necessary for understanding the molecular structure of the H_6^+ cluster. Even in the heavier D_6^+ cluster cation, nuclear fluctuation play an very important role. The present PIMD study suggests that nuclear fluctuation significantly affects the ESR hyperfine coupling constants and the simulation of the ESR parameters using the PIMD formalism [31, 32] should be an important topic in the future. In addition, we hope to perform PIMD simulations of the H_6^+ cluster embedded in large hydrogen clusters in order to understand the environmental effect in solid phase more quantitatively.

Acknowledgements

The authors are grateful to Dr. Takayuki Kumada of Japan Atomic Energy Agency for providing valuable information on their ESR measurements and for useful comments.

References

- [1] S. Yamabe, K. Hirao, K. Kitaura, *Chem. Phys. Lett.* 56 (1978) 546.
- [2] R. J. Beuhler, S. Ehrenson, L. Friedman, *J. Chem. Phys.* 79 (1983) 5982.
- [3] Y. Yamaguchi, J. F. Gaw, H. F. Schaefer III, *J. Chem. Phys.* 78 (1983) 4074.
- [4] H. Huber, *J. Mol. Struct. THEOCHEM* 121 (1985) 281.
- [5] N. J. Kirchner, M. T. Bowers, *J. Phys. Chem.* 91 (1987) 2573.
- [6] Y. Yamaguchi, J. F. Gaw, R. B. Remington, H. F. Schaefer III, *J. Chem. Phys.* 86 (1987) 5072.
- [7] M. Okumura, L. I. Yeh, Y. T. Lee, *J. Chem. Phys.* 88 (1988) 79.
- [8] P. Jungwirth, P. Čársky, *Chem. Phys. Lett.* 195 (1992) 371.
- [9] W. Paul, B. Lucke, S. Schlemmer, D. Gerich, *Int. J. Mass. Spect.* 149 (1995) 373.
- [10] H. Tachikawa, *Phys. Chem. Chem. Phys.* 2 (2000) 4702.
- [11] N. J. Kirchner, J. R. Gilbert, M. T. Bowers, *Chem. Phys. Lett.* 106 (1984) 7.
- [12] N. J. Kirchner, M. T. Bowers, *J. Chem. Phys.* 86 (1987) 1301.
- [13] Y. Eknci, E. L. Knuth, J. P. Toennies, *J. Chem. Phys.* 125 (2006) 133409.
- [14] I. Štich, D. Marx, M. Parrinello, K. Terakura, *Phys. Rev. Lett.* 78 (1997) 3669.
- [15] I. Štich, D. Marx, M. Parrinello, K. Terakura, *J. Chem. Phys.* 107 (1997) 9482.
- [16] Y. Ohta, K. Ohta, K. Kinugawa, *J. Chem. Phys.* 121 (2004) 10991.
- [17] L. R. Wright, R. F. Borkman, *J. Chem. Phys.* 77 (1982) 1938.
- [18] J. A. Montgomery, H. H. Michels, *J. Chem. Phys.* 87 (1987) 771.
- [19] Y. Kurosaki, T. Takayanagi, *Chem. Phys. Lett.* 293 (1998) 59.
- [20] Y. Kurosaki, T. Takayanagi, *J. Chem. Phys.* 109 (1998) 4327.
- [21] M. C. R. Symons, R. G. Wooley, *Phys. Chem. Chem. Phys.* 2 (2000) 217.
- [22] H. U. Suter, B. Engels, S. Lunell, *Adv. Quant. Chem.* 40 (2001) 133.
- [23] T. Kumada, H. Tachikawa, T. Takayanagi, *Phys. Chem. Chem. Phys.* 7 (2005) 776.
- [24] T. Kumada, T. Takayanagi, J. Kumagai, *J. Mol. Struct.* 786 (2006) 130.
- [25] J. Kumagai, H. Inagaki, S. Kariya, T. Ushida, Y. Shimizu, T. Kumada *J. Chem. Phys.* 127 (2007) 024505.
- [26] MOLPRO, a package of ab initio programs, H.-J. Werner and P. J. Knowles,

version 2002.1, R. D. Amos, A. Bernhardsson, A. Berning, P. Celani, D. L. Cooper, M. J. O. Deegan, A. J. Dobbyn, F. Eckert, C. Hampel, G. Hetzer, P. J. Knowles, T. Korona, R. Lindh, A. W. Lloyd, S. J. McNicholas, F. R. Manby, W. Meyer, M. E. Mura, A. Nicklass, P. Palmieri, R. Pitzer, G. Rauhut, M. Schütz, U. Schumann, H. Stoll, A. J. Stone, R. Tarroni, T. Thorsteinsson, and H.-J. Werner.

[27] B. J. Berne, D. Thirumalai, *Ann. Rev. Phys. Chem.* 37 (1987) 401.

[28] M. Shiga, M. Tachikawa, S. Miura, *Chem. Phys. Lett.* 332 (2000) 396.

[29] M. Shiga, M. Tachikawa, S. Miura, *J. Chem. Phys.* 115 (2001) 9149.

[30] M. Shiga, M. Tachikawa, *Chem. Phys. Lett.* 374 (2003) 229.

[31] J. Schulte, M. C. Böhm, R. Ramírez, T. López-Ciudad, *Mol. Phys.* 10 (2005) 105.

[32] R. Ramírez, J. Schulte, M. C. Böhm, *Chem. Phys. Lett.* 402 (2005) 346.

Table 1.Numerical parameters of the analytical function of the H_6^+ potential energy surface

$D_{e1} = 0.13898 \text{ au}$	$D_{e2} = 0.25543 \text{ au}$	$D_{e3} = 0.089843 \text{ au}$
$\alpha_1 = 0.57947 \text{ a}_0^{-1}$	$\alpha_2 = 0.18322 \text{ a}_0^{-1}$	$\alpha_3 = 1.22145 \text{ a}_0^{-1}$
$r_{1e} = 1.64382 \text{ a}_0$	$r_{2e} = 1.89768 \text{ a}_0$	$r_{3e} = 1.49738 \text{ a}_0$
$c_1 = 0.092304 \text{ au}$	$c_2 = 4.2368 \times 10^{13} \text{ au}$	
$\beta_1 = 0.52918 \text{ a}_0^{-1}$	$\beta_2 = 6.35013 \text{ a}_0^{-1}$	$V_e = -4.93803 \times 10^{-2} \text{ au}$

Table 2.

Comparison of harmonic vibrational frequencies (cm^{-1}) of the H_6^+ cluster at the D_{2d} minimum and D_{2h} transition state structures calculated with the fitted potential surface, ab initio CCSD(T), and MP2 methods.

Fit	CCSD(T) ^a	MP2 ^b
D_{2d} minimum		
66.1 (b_1)	172.2	68
356.9 (e)	358.9	365
726.2 (e)	725.3	783
809.2 (a_1)	911.7	904
1086.9 (b_2)	1034.9	1004
891.2 (e)	1187.6	1219
1882.2 (a_1)	2095.3	2089
3785.4 (b_2)	3760.6	3865
3785.9 (a_1)	3838.9	3941
D_{2h} transition state		
65.4 i (a_u)	50.6 i	91 i
350.5 (b_{2u})	340.2	345
387.0 (b_{3u})	390.2	396
647.2 (b_{3g})	613.1	674
824.8 (a_g)	841.1	905
826.2 (b_{2u})	907.7	934
847.0 (b_{1u})	1031.8	1004
913.9 (b_{2g})	1075.5	1084
1085.7 (b_{3g})	1245.0	1288
1879.4 (a_g)	2096.3	2091
3786.9 (b_{1u})	3771.3	3868
3788.0 (a_g)	3851.3	3945

^aPresent ab initio calculation at the CCSD(T)/cc-pVTZ level

^bMP2/ cc-pVTZ-level calculation taken from ref. 20.

Figure Captions

Fig. 1 Comparison of the potential energy profiles along several internal coordinates obtained from the ab initio electronic structure calculation at the CCSD(T)/cc-pVTZ level (circles) and the fitted potential energy surface (solid lines). Definition of the internal coordinates used in these plots is also shown. R_1 is the internuclear distance between the central two H atoms, R_2 is the distance between the central H atom and the midpoint of the outer H₂, and R_3 is the internuclear distance between outer two H atoms. ϕ is the dihedral angle of outer H₂ nuclei.

Fig. 2 Three-dimensional perspective plots of probability distribution functions of the H₆⁺ nuclei (a) and D₆⁺ nuclei (b) obtained from the PIMD simulation at $T = 4$ K. Right panels, (c) and (d), show the corresponding probability distributions projected onto the yz plane.

Fig. 3 One-dimensional probability density distributions as a function of the dihedral angle ϕ (a) and the displacement distance d (b). Definition of these two coordinates is also shown (The displacement distance d is the projected distance measured from the line connecting two midpoints of the outer H₂ molecules). Potential energy profile as a function of ϕ is also plotted as a bold solid line in (a).

Fig. 4 Schematic representation of the atomic displacement vectors for lower vibrational frequencies for the H₆⁺ cluster at D_{2d} and D_{2h} configurations.

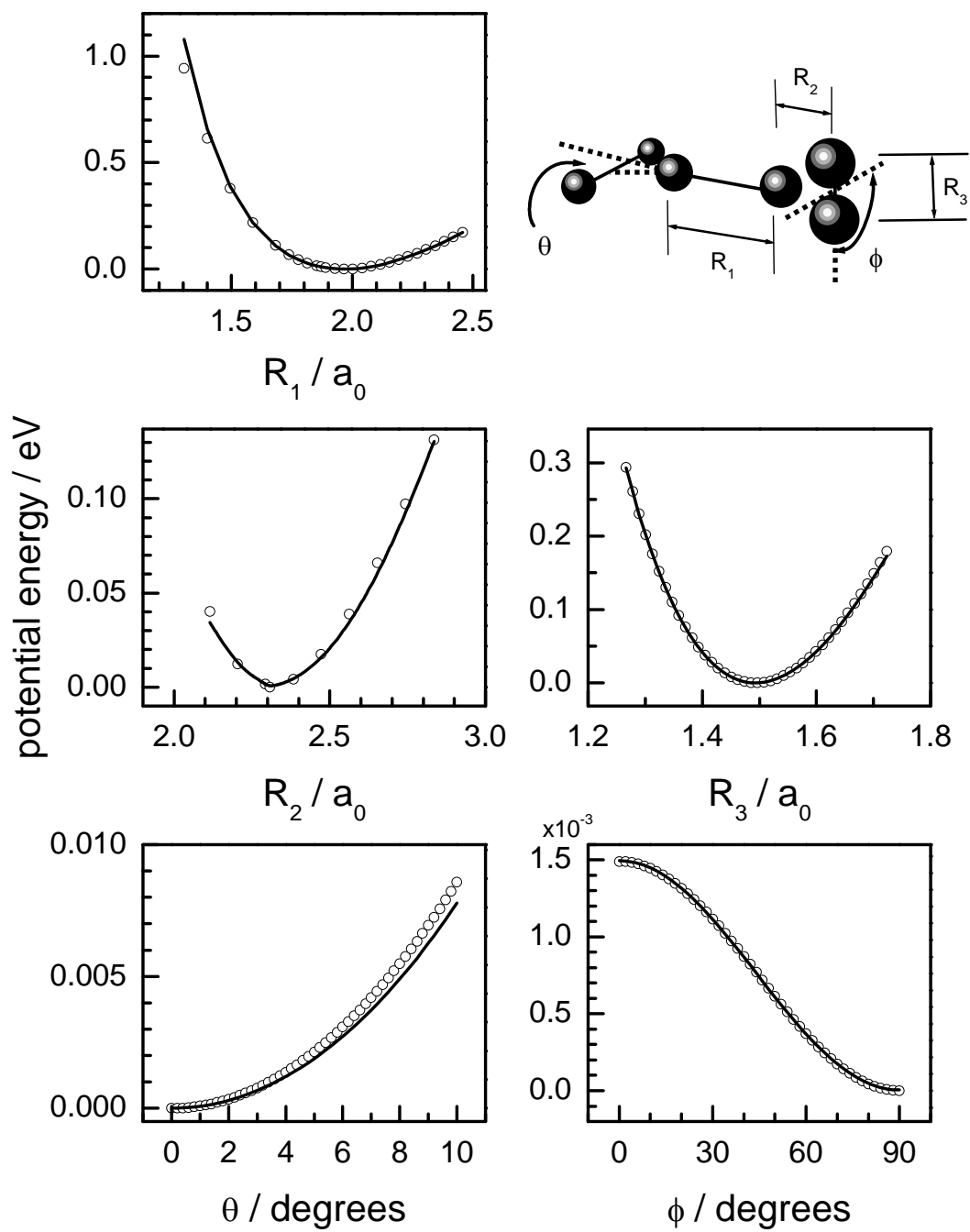


Figure 1

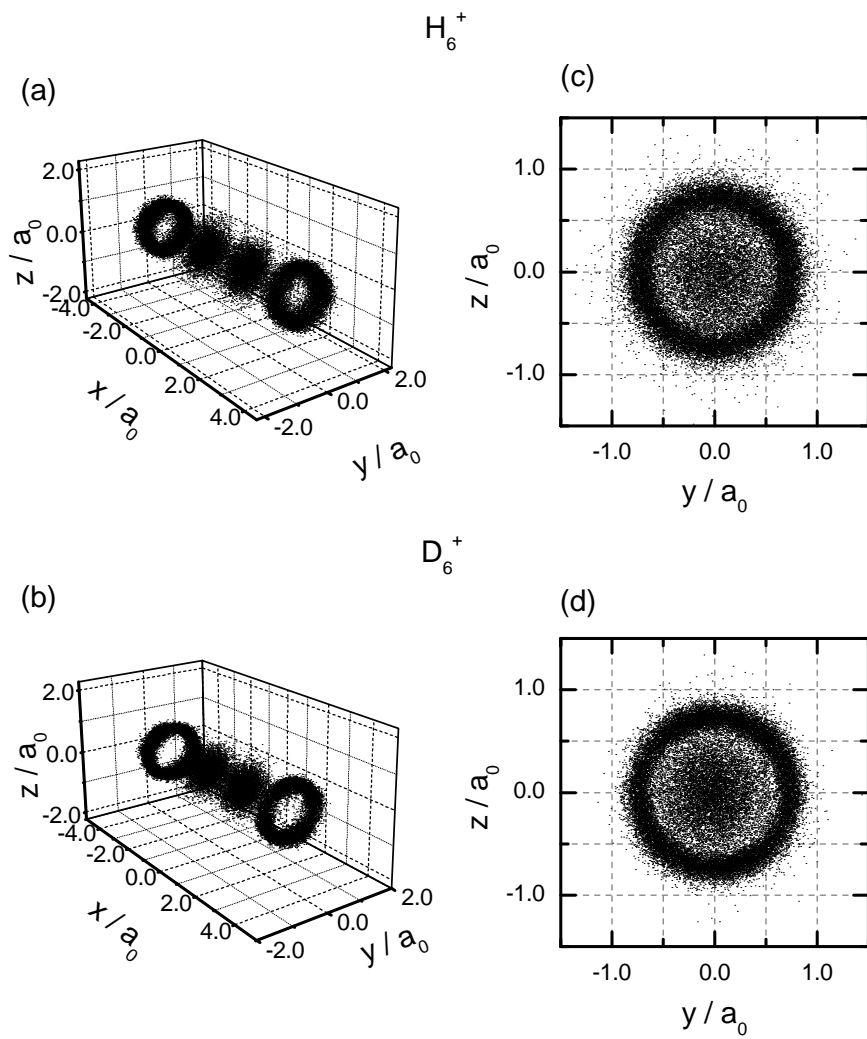


Figure 2

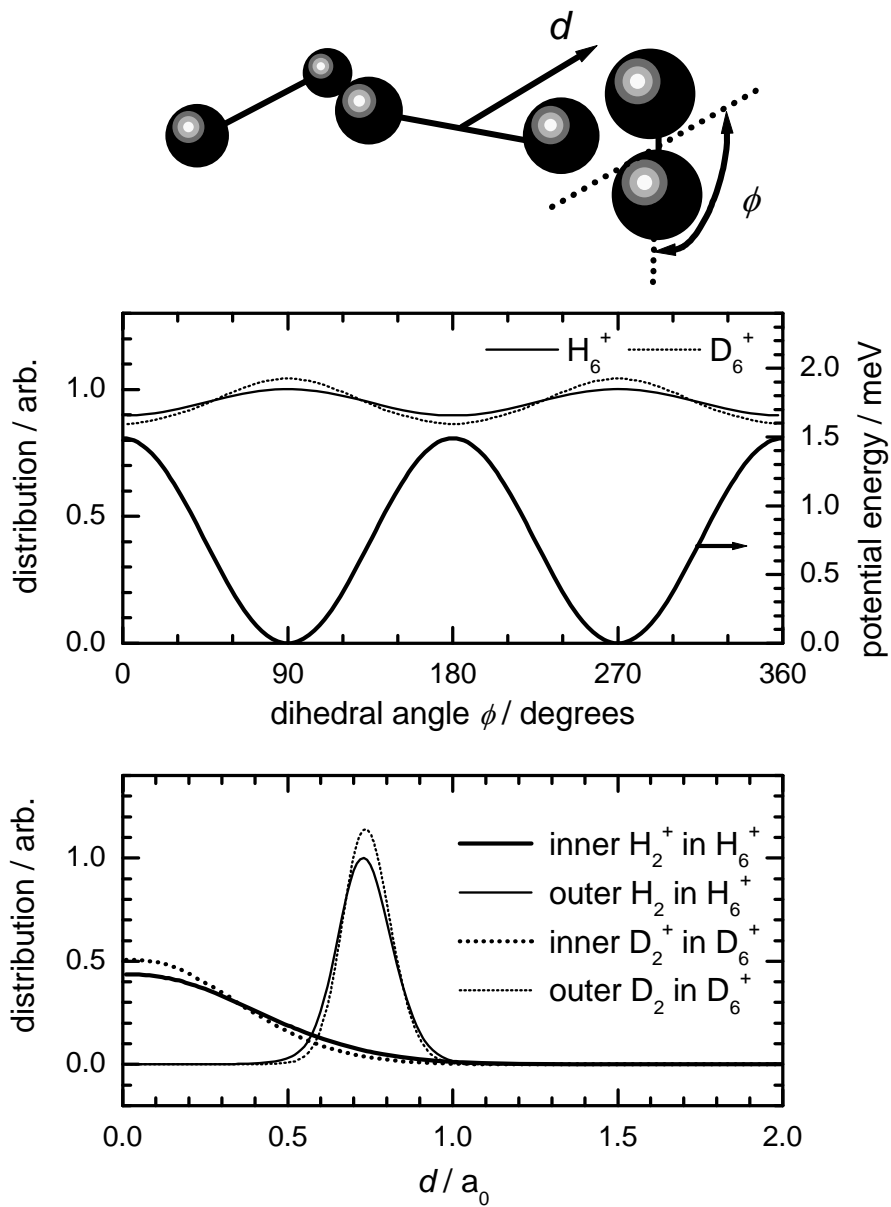


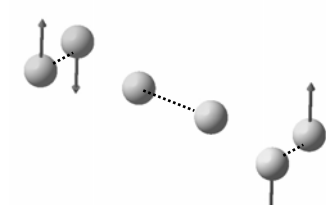
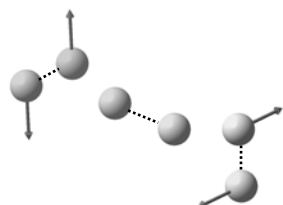
Figure 3

D_{2d} minimum

D_{2h} transition-state

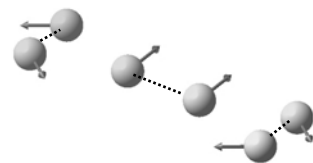
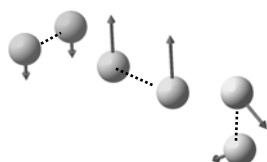
(a) 66.1 cm^{-1} (b_1)

(d) 65.4 i cm^{-1} (a_u)



(b) 356.9 cm^{-1} (e)

(e) 350.5 cm^{-1} (b_{2u})



(c) 356.9 cm^{-1} (e)

(f) 387.0 cm^{-1} (b_{3u})

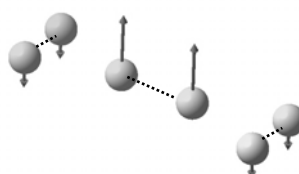
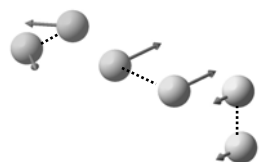


Figure 4